(article starts on next page)

Subsea tunnel reinforced sprayed concrete subjected to deterioration harbours distinct microbial communities

Sabina Karačić, Britt-Marie Wilén, Carolina Suarez, Per Hagelia & Frank Persson

View supplementary material

Published online: 10 Feb 2019.

Submit your article to this journal

Article views: 283

View Crossmark data

Taylor & Francis
Taylor & Francis Group

Subsea tunnel reinforced sprayed concrete subjected to deterioration harbours distinct microbial communities

Sabina Karačić[a], Britt-Marie Wilén[a], Carolina Suarez[b], Per Hagelia[c] and Frank Persson[a]

[a]Department of Architecture and Civil Engineering, Chalmers University of Technology, Göteborg, Göteborg, Sweden; [b]Department of Chemistry and Molecular Biology, University of Gothenburg, Göteborg, Göteborg, Sweden; [c]Tunnel and Concrete Division, The Norwegian Public Roads Administration, Oslo, Norway

ABSTRACT

Deterioration of concrete is a large societal cost. In the Oslofjord subsea tunnel (Norway), deterioration of sprayed concrete and corrosion of reinforcing steel fibres occur under biofilm formed at sites with intrusion of saline groundwater. In this study, the microbial community structure, *in situ* environmental gradients and chemical composition of the biofilms were examined at three tunnel sites. Ammonia- and nitrite-oxidising microorganisms, in particular *Nitrosopumilus* sp., and iron-oxidising bacteria within *Mariprofundus* sp., were omnipresent, together with a diversity of presumably heterotrophic bacteria. Alpha- and beta diversity measures showed significant differences in richness and community structure between the sites as well as over time and null-models suggested that deterministic factors were important for the community assembly. The superficial flow of water over the biofilm had a strong effect on oxygen penetration in the biofilm and was identified as one major environmental gradient that varied between the sites, likely being important for shaping the microbial communities.

Introduction

Biodeterioration of concrete caused by the metabolic activities of microorganisms, including bacteria, archaea, fungi and algae, results in significant societal problems with a large worldwide economic impact (Gaylarde and Morton 1999). The deterioration of concrete leads to undesirable changes in concrete structure and function due to changes in the material components, including cracking, spalling, pitting and leaching of compounds from the concrete matrix (Cwalina 2008; Harbulakova et al. 2013). For biodeterioration to occur, microbial colonisation and biofilm formation is needed, a process referred to as biofouling. Formation of biofilms provides several advantages for their community members such as easy access to nutrients, and resistance to extreme environments and aggressive compounds. In the biofilm, the microbial cells are embedded in self-produced extracellular polymeric substances (EPS). Mature biofilms are highly hydrated and open structures with void spaces between colonies of diverse microorganisms creating gradients of microenvironments (Stoodley et al. 1999; Okabe et al. 2007). Concrete surfaces provide favourable conditions for biofouling due to their high roughness

with pores and microcracks (Hughes et al. 2013). After construction, concrete is immune to microbial colonisation because of the high alkalinity, with pH in the range of 11–13. Biofouling occurs once the pH has dropped to 9–10, due to carbonation caused by the presence of carbon dioxide (Bastidas-Arteaga et al. 2008). Microbial growth and succession of the biofilms formed on the concrete further reduces the pH due to the release of biogenic acids such as carbonic acid, nitric acid, hydrogen sulphide and sulphuric acid, which eventually dissolve the cement paste matrix (Okabe et al. 2007; Peyre Lavigne et al. 2015). However, the biogenic acids alone cannot explain the full deterioration of concrete, which is rather an effect of ongoing microbial interactions (Magniont et al. 2011). The decreased pH also promotes corrosion of the reinforcing steel bars and fibres (Taylor 1997). Steel corrosion is furthermore accelerated by the EPS in the biofilms, which contain negative charges that promote ionic- and electrostatic binding with metals creating galvanic reactions (Beech and Sunner 2004).

In the marine environment, biodeterioration of concrete structures is a widespread problem, for instance

of pipelines and off-shore infrastructure in the oil and gas industry (Noeiaghaei et al. 2017). In seawater, biodeterioration is complex and occurs in conjugation with abiotic processes including carbonation, chlorine ingress and sulphate attack. These processes increase concrete permeability, which reduces the concrete strength and facilitates cracking. Increased concrete porosity can furthermore result in deep corrosion of the concrete reinforcement (Torres-Luque et al. 2014). Unlike in sewers systems, where the general microbial mechanisms for deterioration are thoroughly investigated (Noeiaghaei et al. 2017), little is known about the biological interactions leading to biodeterioration of concrete infrastructure in the marine environment.

A novel case of biodeterioration of fibre reinforced sprayed concrete used for rock support has been detected in some Norwegian subsea tunnels (Hagelia 2007). Previous research, mainly focusing on the Oslofjord subsea tunnel, has shown that degradation of the cement paste matrix was due to a combined biotic and abiotic attack. Biofilms of iron-rich dark rusty to orange slime and manganese-rich dark material, associated with saline leakages on the rough and tortuous sprayed concrete surfaces, had caused variably deep disintegration of the calcium silicate hydrate (C-S-H). This effect was at least partly due to acidification (pH 5.5–6.5) of saline tunnel waters (pH 7.5–8) caused by chemical reactions within the biofilms. A multiproxy study, involving concrete petrography, scanning electron microscopy (SEM), microchemical analysis, X-ray diffraction, water chemical analysis and stable carbon and sulphur isotopes, demonstrated that reactions within the biofilm were influenced by biomineral formation and redox reactions, being sensitive to growth of biota. The biofilms interacted with the iron, manganese, sulphur, carbon and nitrogen cycles. Carbonates such as calcite, aragonite and magnesite occurred in degraded concrete underneath biofilm in the presence of biominerals (Mn-oxides buserite and todorokite and ferrihydrite). Reduction of Mn, Fe and S took place in

thick biofilms involving temporary formation of sulphide. The evidence suggests that acidification within the biofilm was caused by oxidation of Fe(II) and Mn(II), sulphuric acid formed by reoxidation of sulphides, redox reactions between Fe and Mn compounds and organic acids. Microorganisms visible under SEM resembled *Gallionella* or *Mariprofundus* and *Leptrohrix discophora*, associated with manganese oxides. The abiotic attack mainly affected the concrete adjacent to the rock mass, being characterised by calcium leaching, breakdown of portlandite, magnesium attack and thaumasite sulphate attack and transformations of the cement paste matrix in response to ion-rich water. Further details may be found in Hagelia (2011a).

However, basic knowledge about the specific role of the community structure of the microbial biofilms in the subsea tunnels, as well as of biofilms on related concrete structures in marine environments, is lacking. In order to understand and ultimately prevent deterioration processes caused by microbial activity, such knowledge is pivotal. In this study high throughput amplicon sequencing of 16S rRNA genes was used to assess the composition, diversity and community assembly of microbial biofilms at three sites subjected to concrete deterioration in the Oslofjord subsea tunnel. The chemical microenvironment within the biofilm was measured *in situ*, using oxygen and pH microelectrodes, as well as measurement of the chemical composition of water and biofilm with the aim of providing a linkage between the biofilm community structure and the environmental conditions.

Materials and methods

Site description

Sampling was performed in the Oslofjord subsea road tunnel near Drøbak, Norway (59°39′53″N 10°36′47″E/ 59.66472°N 10.61306°E, Figure S1). The Oslofjord tunnel is 7,306-m long with a width of 11.5 m reaching a maximum depth of 134 m below the sea level (Figure 1). The rock mass mainly consists of granitic
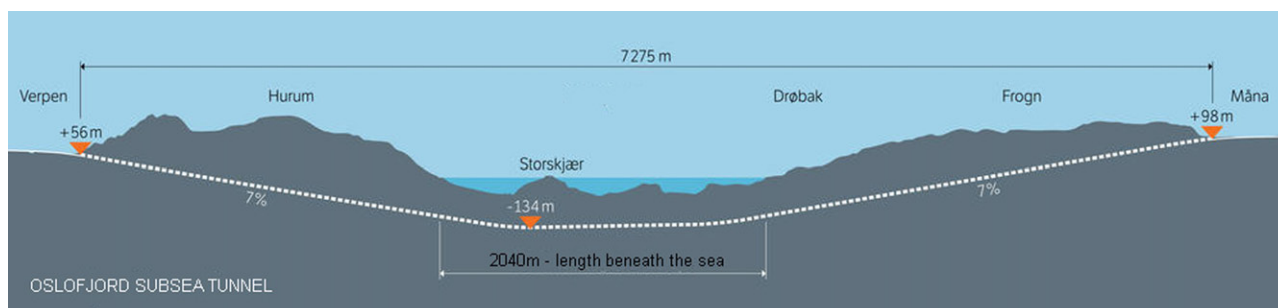

Figure 1. Overview of the Oslofjord showing the tunnel length and depth/height relative to the sea level.

gneiss and pegmatite with joints and fault zones carrying clay minerals. Biofilm samples were collected from three different tunnel localities: the Main Tunnel, the Pump Station and the Oslofjord Test Site (Figures S2 and S3), representing two different concrete substrata. (1) The concretes at the Main Tunnel and the Pump Station were sprayed in 1999 as permanent rock support. These concretes were based on a rapid setting cement (CEM I) with water/binder-ratio = 0.42, a binder content about 514 eq kg m^{-3}, 5% silica fume (by cement weight), steel fibre reinforcement and superplasticers. The concretes represent Durability Class M45 and Strength Class B45 according to the concrete standard NS EN 206. Al-sulphate was used as setting accelerator. (2) The Oslofjord Test Site for sprayed concrete durability was established by the Norwegian Public Roads Administration in March 2010. Soon after the site establishment, microbial biofilms were observed (Hagelia 2011b). The concrete at the Test Site was based on CEM II/AV 42,5 R (eg with ~18% fly ash), and otherwise prepared with different mixes. The biofilm sampling stations are located on sprayed concretes made with water/binder ratio = 0.43, 4% silica fume, superplactisiser and both steel fibres and polypropylene fibres. Al-sulphate was used as setting accelerator. The concrete corresponds to M45 and B45, similar to the two other sites. However, concrete made with fly ash cements are regarded as more durable than those based on CEM I. The NS EN 206 Exposure Class, to assess risks for cement paste degradation and steel fibre corrosion, was XC2-XC3, XS3, XA3 at all three investigated sites and all concrete mixes used are regarded as durable in such an environment (see Tables S1 and S2 for an overview of the EN 206 exposure classification). However, it should be noted that the standard environmental classification for concrete does not account for the effects of biofilms (Hagelia 2011a; Bertron 2014).

The water temperatures were 13 °C at the Pump Station and 8–9 °C at the Main Tunnel and Test Site locations, being fairly constant over several years. The water flow rates associated with biofilms were not measured, but were mainly characterised by slowly seeping waters at all locations. It should, however, be noted that the water load at the Pump Station increased permanently in 2013, both spatially and volumetrically. In contrast, water flow during the preceding 13–14 years was characterised by slowly seeping waters sustaining biofilm formation in a much smaller area.

Sampling and chemical analysis

Biofilm samples for microbial community analysis were collected from the three tunnel sites on three occasions: November 2015, March 2016 and October 2016. Core samples of the thick and soft biofilm (10–15 mm thickness) were collected using metallic tubes, whilst thin biofilms were scraped off the concrete with a scalpel. The biofilm samples were snap-frozen in an ethanol–dry-ice mixture immediately at sampling, kept in dry ice during transportation, and stored at –80 °C until nucleic acid extraction. A subset of the biofilm samples was also used for chemical analyses (see below). The water samples for chemical analyses were collected in 500 ml sterile bottles and stored in dry-ice during transportation to the laboratory. All water samples were filtered (0.45 µm) before analysis. The biofilm samples for chemical analysis were homogenised and dried at 105 °C prior to analysis. Selected metals from water and biofilm samples were quantified by quadrupole Inductively Coupled Plasma-Mass Spectrometry (ICP-MS) using a iCAP Qc (Thermo Fisher Scientific, Wilmington, DE, USA) after microwave digestion, using HNO_3, following the EPA 3051 protocol for ETHOS EASY system digestion. Total solids (TS) and volatile solids (VS) of the biofilms were analysed according to APHA 1998 Standard Methods 2490 A-D. Chloride, nitrate, ammonium and sulphate in the water were analysed according to FINAS accreditation methods (RA2018, RA2046).

DNA extraction, PCR, sequencing and data analysis

A full description of the workflow, including bioinformatics, is found in the Supplemental material. Briefly, DNA was extracted from 500 mg of biofilm using the Fast DNA spin kit for soil (MP Biomedicals, Santa Ana, CA, USA) and the 16S V4 region of the rRNA gene was amplified by PCR using the primers 515′F and 806 R, to cover both bacteria and archaea (Caporaso et al. 2011; Hugerth et al. 2014). After purification and normalisation, the pooled PCR products were sequenced on an Illumina MiSeq using the MiSeq Reagent Kit v2 (Illumina Inc., San Diego, CA, USA). Sequence processing and curation was performed using USEARCH v.10 (Edgar 2010) with classification to the MiDAS curated database (McIlroy et al. 2015). Putative functions of the classified sequence variants (SVs) were assigned according to literature. Sequence reads were deposited at the NCBI Sequence Read Archives, Bioproject PRJNA481470, accession numbers SAMN09669680-SAMN09669744.

Multivariate statistics; diversity- and null-model calculations; and data visualisation were conducted within the R packages ampvis 1.14 (Albertsen et al. 2015), vegan 2.5.1 (Oksanen et al. 2017) and picante 1.6.2 (Kembel et al. 2010). Beta diversity was estimated using pairwise Sørensen and Bray–Curtis dissimilarities and visualised using principal coordinate analysis (PCoA). Differences in beta diversity were tested for using permutational multivariate analysis of variance (PERMANOVA). The standardised effect size (SES) for pairwise Sørensen dissimilarities was estimated in vegan to test for stochastic community assembly, with a null-model that preserves species richness and species incidence, using the quasiswap algorithm, with settings thin = 1,000 and 999 simulated null-communities. Unweighted nearest taxon index was estimated using picante with the null-model "taxa.labels" at 999 iterations to test for phylogenetic clustering among closely related taxa. Possible links between the microbial community structure and the chemical properties of the biofilm and the water were explored with environmental fitting (envfit, 999 permutations) to PCoA ordinations based on Sørensen dissimilarities in vegan. Differences in community richness and evenness were tested for using Welch's ANOVA followed by *post hoc* analysis using the Games-Howell test.

Microsensor measurements

In situ gradient measurements of oxygen and pH in the biofilms were performed from the biofilm–water interface towards the substratum. The Clark-type oxygen microsensor (tip diameter 50 μm; OX-50, Unisense, Aarhus, Denmark) was calibrated with 100% air-saturated saline groundwater at the prevailing temperature in a calibration chamber (CAL300) following the manufacturer's protocol. The pH microsensor (tip diameter 50 μm, linear range pH 4–9; pH-50, Unisense), used in combination with a reference electrode (tip diameter of 50 μm; REF-50, Unisense), was linearly calibrated with three pH buffer points (pH 4, 7 and 9) at the prevailing temperature. Microelectrodes were connected to a field microsensor multimeter (Unisense); fixed in a motorised micromanipulator (MM33-2, MC-232; Unisense A/S); and controlled by the software SensorTrace PRO (Unisense A/S). Prior to each measurement, the biofilm depth was estimated using a spent microsensor. The microsensor tip was positioned at the biofilm–water interface, defined as the starting position (0 μm on graphs), by means of the micromanipulator and microprofiling was conducted in steps of 500 μm with a waiting period before each measurement of 10 s.

Scanning electron microscopy (SEM)

Uncoated handpicked samples were mounted on carbon tape. Chemical point analyses (1–2 μm^2) were performed on pristine untreated samples, using a Hitachi S-4800SEM with energy-dispersive X-ray spectroscopy (EDS, Noran System SIX, Thermo Fischer Scientific, Wilmington, DE, USA). The instrument was operated at accelerating voltage, 15 kV, at high vacuum. Analytical accuracy for most elements is within 1–2% (w w^{-1}) with somewhat less accuracy for carbon and nitrogen. Back scatter electron images were also captured.

Results

Water and biofilm chemistry

The saline groundwater from the Oslofjord subsea tunnel had a general composition similar to seawater, with high concentrations of chloride (20–22 g l^{-1}), sodium (10 g l^{-1}) and sulphate (2.7–3.3 g l^{-1}), and low concentrations of ammonium (<0.3–0.7 mg l^{-1}), nitrate (3.0 mg l^{-1}) and dissolved organic carbon (<1.5 mg l^{-1}). In a campaign, water samples were taken from both water that flowed through rock mass without interaction with the concrete and from water after interaction with the concrete and associated biofilm. Calcium, magnesium and vanadium concentrations were higher in the water that had been in contact with biofilm and concrete, compared to the water that had only been in contact with the rock mass for all (Ca) or 5/6 (Mg, V) of the comparisons (Table 1), while for the other elements, no apparent differences were detected.

The chemical composition of the biofilm is shown in Table 2. Sampling points for the biofilm are shown in Figure S3. Relatively high concentrations of iron and calcium were detected in orange samples while black biofilm samples contained relatively high concentrations of manganese. The loss on ignition, as a measure of organic matter content of the biofilm, was 12.6 ± 0.7% (average ± SD), indicating that most of the biofilm components were inorganic.

Biofilm community composition

Taxonomic analysis of the 16S rRNA SVs showed that members of the phylum Proteobacteria were predominant, representing 44-49% of the total biofilm community. Besides Proteobacteria the majority of

Table 1. Chemical composition of the water samples taken after contact with biofilm and concrete (WCB) or only in contact with rock mass (WR) from the three sites.

Site		Pump Station		Pump Station		Pump Station		Test Site		Test Site		Main Tunnel	
Year		2015		2016		2016		2016		2017		2017	
Water type		WCB	WR	WCB	WR	WCB	WR	WCB	WR	WCB	WR	WCB	WR
Mg	mg l^{-1}	2,232	1,147	1,323	1,202	1,150	821	1,416	1,400	1,121	1,224	1,880	1,291
Al	mg l^{-1}	0.356	0.673	0.319	0.378	0.328	0.352	0.646	0.381	0.531	0.392	0.781	0.558
Ca	mg l^{-1}	604	292	343	297	274	236	362	314	384	361	513	486
Ti	mg l^{-1}	0.96	0.848	1.009	0.887	0.815	0.783	0.993	0.898	0.618	0.675	0.826	0.821
V	mg l^{-1}	0.26	0.127	0.146	0.132	0.126	0.114	0.16	0.155	0.144	0.158	0.216	0.152
Cr	mg l^{-1}	0.015	0.009	0.011	0.212	0.007	0.007	0.016	0.01	0.01	0.01	0.01	0.01
Mn	mg l^{-1}	1.32	1.28	1.31	1.28	1.03	1.28	1.36	1.54	2.11	1.7	1	1.09
Fe	mg l^{-1}	0.01	0.01	0.01	0.01	0.01	0.01	0.02	0.02	0.17	0.17	0.01	0.02
Co	mg l^{-1}	0.003	0.002	0.002	0.004	0.001	0.005	0.003	0.002	0.002	0.003	0.003	0.003
Ni	mg l^{-1}	0.747	0.247	0.784	0.942	0.809	1.198	1.559	1.229	0.004	1.161	5.324	0.028
Cu	mg l^{-1}	0.42	0.266	0.337	0.398	0.294	0.462	0.495	0.476	0.233	0.456	0.231	0.883
Zn	mg l^{-1}	1.025	0.801	1.072	5.983	1.141	3.382	3.377	3.249	0.091	3.241	0.243	4.77
Cd	mg l^{-1}	0.001	0.002	0.001	0.002	0.001	0.002	0.002	0.002	0.006	0.004	0.002	0.009
Pb	mg l^{-1}	0.032	0.037	0.039	0.082	0.048	0.172	0.097	0.125	0.068	0.167	0.32	0.006

Table 2. Chemical composition of the biofilms sampled in 2017.

Site		Pump Station		Test Site				Main Tunnel		
Sampling points		P1	P2	T1F1	T1F1 top	T2F2	T2S2	M2S3	M1S3	M2S2
Biofilm description		Black	Orange	Orange	Orange/Black	Orange/Black	Black	Black	Orange/Black	Black
Mg	mg g^{-1}	23.04	36.97	39.65	17.77	14.2	17.14	29.19	27.75	2.4
Al	mg g^{-1}	2.91	0.55	2	1.58	1.25	1.94	14.56	13.69	0.72
Ca	mg g^{-1}	29.68	30.94	38.2	22.1	20.84	23.24	17.85	50.47	6.99
Mn	mg g^{-1}	284.07	260.84	74.83	89.95	132.97	225.49	40.56	38.74	32.9
Fe	mg g^{-1}	157.19	538.2	792.33	209.58	246.29	103.57	23.32	17.75	17.31
Ti	mg g^{-1}	0.19	0.09	0.21	0.13	0.06	0.13	1.14	1.03	0.01
Cr	mg g^{-1}	nd*	nd	nd	0.01	nd	nd	0.03	0.03	nd
Co	mg g^{-1}	0.01	0.03	nd	0.02	0.01	0.01	0.02	0.02	nd
Ni	mg g^{-1}	0.33	0.11	0.24	0.18	0.08	0.07	0.07	0.08	0.19
Cu	mg g^{-1}	0.09	0.07	0.25	0.16	0.15	0.04	0.14	0.15	0.08
Zn	mg g^{-1}	0.5	0.79	0.61	1.06	0.51	0.53	2.46	0.36	0.4
Pb	mg g^{-1}	0.05	0.04	0.09	0.07	0.07	0.04	0.04	0.04	0.03
TSS	g l^{-1}	240	219	220	280	363	350	166	131.8	93
Loss on ignition	%	11.7	13.8	12.8	12.76	13.56	12	11.87	12.59	12.3

The sampling points are illustrated in Figure S3.
*Not detected.

the SVs belonged to Planctomycetes, Thaumarchaeota, Bacteroidetes and Actinobacteria. In addition, Acidobacteria and Nitrospirae were present with relative sequence abundance >2% of the total communities in the 64 biofilm samples (Figure 2).

The top 25 SVs from the three different tunnel sites are shown in Figure 3. Many of the SVs were affiliated to autotrophic nitrogen converting microorganisms. The most abundant microorganism was the ammonia-oxidising archaeon *Nitrosopumilus* sp. with an average relative sequence read abundance of 17% across all samples. Also, betaproteobacterial ammonia-oxidising bacteria within the Nitrosomonadaceae were common in the biofilm (average relative abundance of 2.5%). SVs affiliated to the marine nitrite-oxidising bacterium *Nitrospina* sp. were present at average abundance of 2.0% with several samples having >10% relative abundance. Nitrite-oxidising or completely nitrifying *Nitrospira* sp. were present at an average relative abundance of 1.2%, as were anammox bacteria within *Candidatus* Scalindua sp. Furthermore, the iron-oxidising bacterium *Mariprofundus* sp. was detected at high relative abundance (>10%) in a few samples with an average relative abundance of 2.0%. Several SVs were furthermore assigned to putative heterotrophic bacteria within the Saprospiraceae (2.9% average relative abundance), the marine benthic group JTB255 (1.3%), Kordiimonadaceae (1.3%) and *Marinicella* (1.9%).

Biofilm diversity and community assembly

Alpha diversity was measured as taxonomic richness (observed number of SVs) and evenness (Simpson's) for the biofilm communities from the three tunnel sites (Figure 4). The richness was significantly different between the sites (Welch's ANOVA, $p < 0.001$),
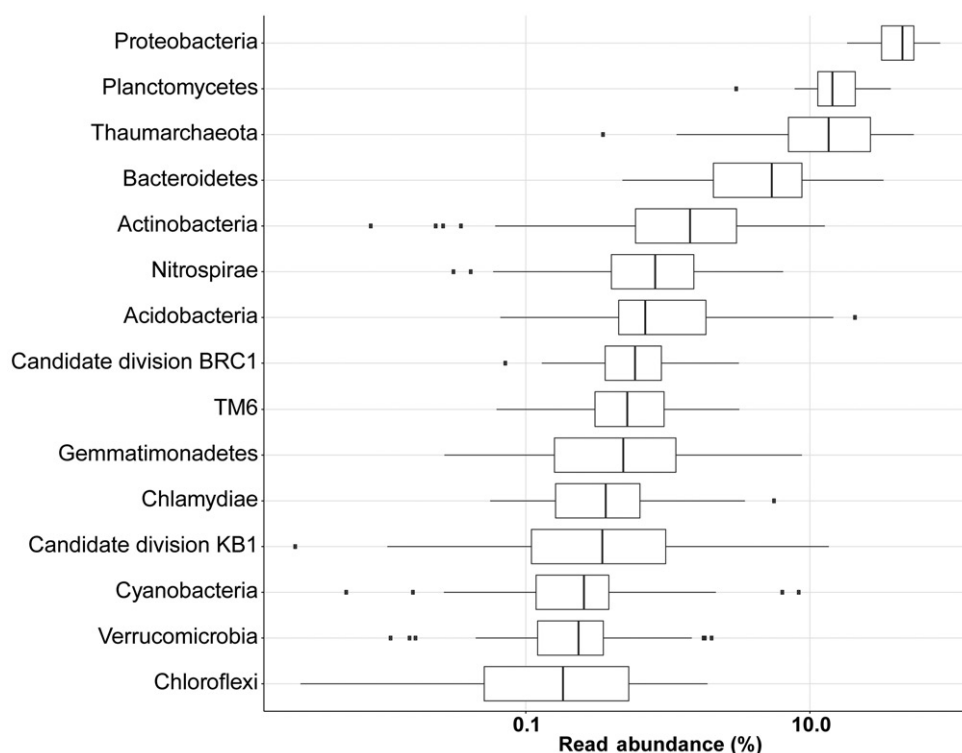
Figure 2. Boxplot showing the top 15 major phyla in the biofilms. Read abundance (x-axis) is displayed on a log-scale. The boxplot depicts the median (vertical bold line); 25th and 75th percentiles (box delimiters); minimum and maximum values excluding outliers (horizontal lines); and outliers (dots).

with the Pump Station having significantly lower richness than the Test Site (*post hoc*, Games–Howell, $p < 0.001$). However, evenness was rather similar between the sites with no significant differences.

The beta diversity of the biofilm communities from the three tunnel sites across all three sampling occasions was visualised with PCoA based on Sørensen dissimilarities (Figure 5). The three sites clearly separated in community structure. Slightly less pronounced separation was observed based on Bray–Curtis dissimilarities, which put a large weighting on the abundant community members (Figure S4). The separation between sites was confirmed by PERMANOVA for both dissimilarities based on Sørensen and Bray–Curtis, showing that the three sites were significantly different from each other in community structure (Tables 3 and S3). In addition, clear temporal dynamics of the microbial communities from November 2015 to October 2016 was observed at the Pump Station, while for the Test Site and the Main Tunnel, no significant changes were observed (Tables 3 and S3).

To assess the variations in beta diversity independent of the variations in alpha diversity, and thereby also to assess the effect of stochasticity on the microbial community assembly, null-models were used.

Analysis based on standard effect size (SES) showed that within each site, SES was similar to, or lower than, two SDs from the null-model predictions of random community assembly, while between sites, SES were similar to or higher than two SDs from the null-model predictions (Figure 6). Furthermore, analysis using nearest taxon index indicated significant phylogenetical clustering among closely related taxa within the microbial communities at each site (Figure S5).

The biofilm chemical composition could not explain the observed microbial community structure, as assessed by environmental fitting (Table S5). Neither could the chemical composition in the water coming from the rock mass (Table S4). However, for the water samples in contact with the biofilm and concrete, calcium, magnesium and vanadium displayed a significant fit to the ordination (Table S4).

Microscopic analysis of biofilm

SEM-EDS point analysis of biofilm sampled in 2016 (Figure 7) showed twisted stalks (points 1 and 2), suggesting the presence of the marine iron-oxidising bacterium *Mariprofundus* sp., as well as non-specified biomass (points 3 and 4) and anticipated mineral
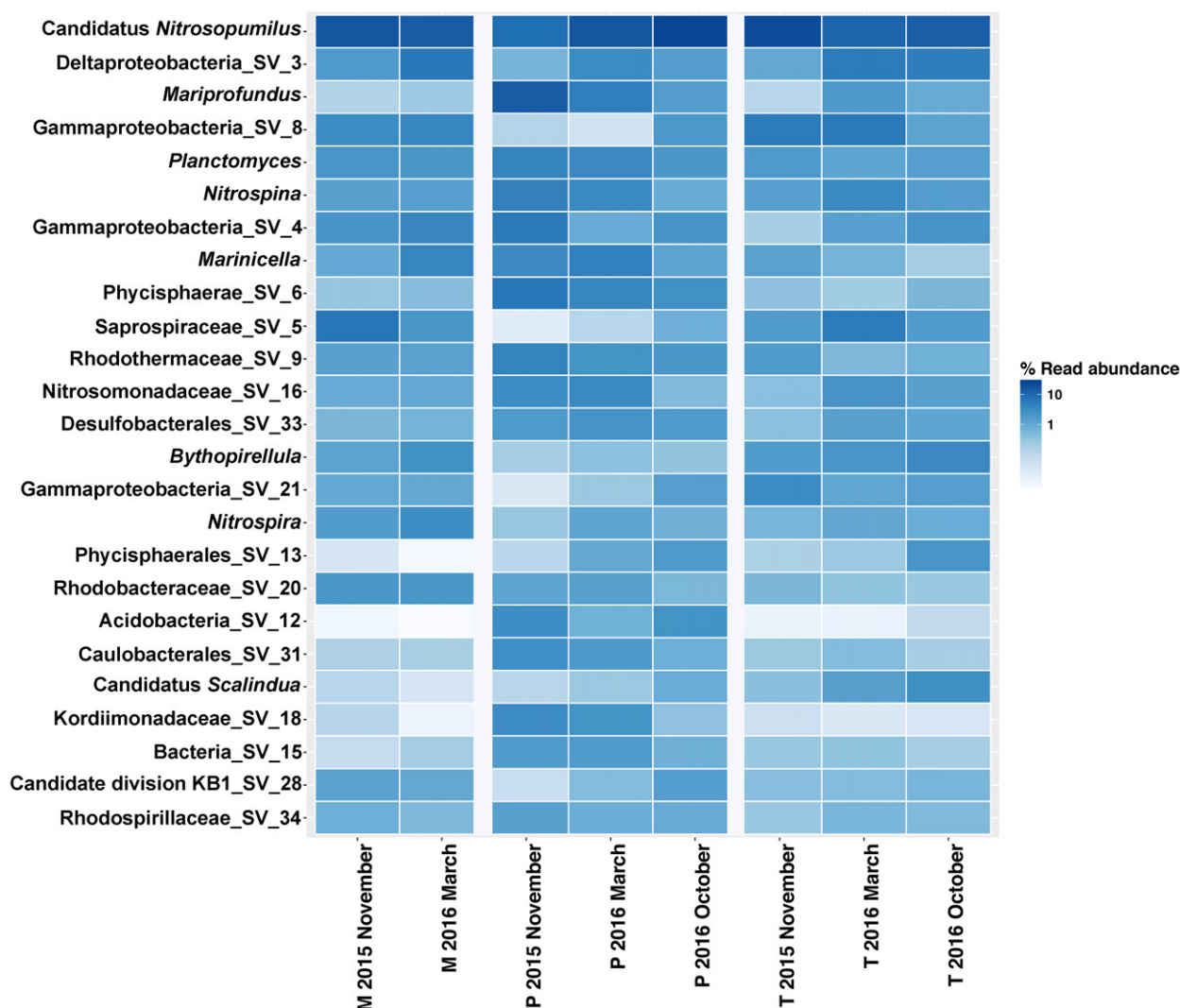
Figure 3. Heatmap showing the 25 most abundant SVs in the biofilm at the Main Tunnel (M), Pump Station (P) and the Test Site (T). Abundance data show average values at each sampling occasion (November 2015, March 2016 and October 2016).

material (point 5). Results from the EDS analysis of points 1–5 are shown in Table 3. Besides oxygen and carbon, expected to be found in organic material, the stalks (points 1 and 2) were particularly rich in iron. Even the non-specified biomass (points 3–4) contained a lot of iron compared to the mineral material (point 5), which had a Si/O-ratio of 0.5, confirming this was quartz with associated biogenic carbon.

Biofilm *in situ* gradients of pH and dissolved oxygen

Microsensor profiling of pH and concentrations of dissolved oxygen (DO) was performed at the Pump Station site, at several local spots. The measured DO profiles revealed differences among local spots which varied in their superficial water flow rate. With high superficial water flow rate, DO decreased at a lesser extent with biofilm depth than at lower superficial water flow rate (Figure 8). The largest differences in DO concentrations were measured in biofilm with only slight dripping of water across the biofilm surface. Here DO decreased from 9 mg l^{-1} at the biofilm–water interface to below 3 mg l^{-1} in the inner biofilm regions close to the concrete (as measured by penetrating a sacrificial microsensor into the concrete). In contrast to DO, only slight changes in pH were observed with increasing biofilm depth, typically from a pH ~8.2 at the biofilm–water interface to 7.7 in the inner biofilm regions (Figure S6).

Discussion

Deterioration of the subsea tunnel reinforced sprayed concrete is a complex phenomenon caused by biotic and abiotic interactions which result in breakdown of
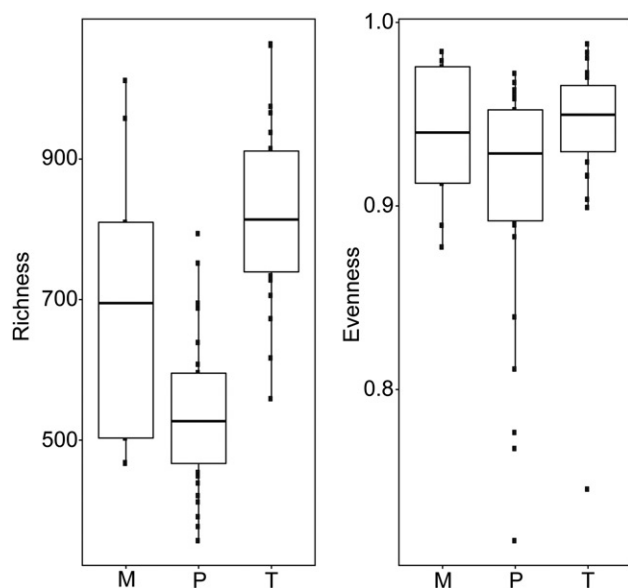
Figure 4. Richness (observed number of SVs) and evenness (Simpson's) of the microbial communities at the Main Tunnel (M), Pump Station (P) and the Test Site (T). The boxplot depicts the median (horizontal bold line); 25th and 75th percentiles (box delimiters); minimum and maximum values excluding outliers (vertical lines); and outliers (dots).
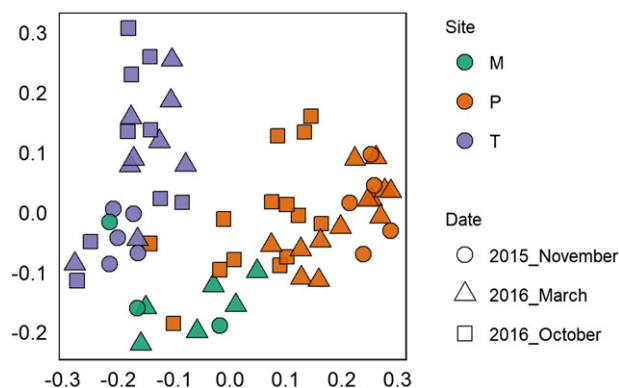

Figure 5. PCoA ordination based Sørensen dissimilarities across the three sampling occasions of the microbial communities at the Main Tunnel (M), Pump Station (P) and the Test Site (T).

Table 3. PERMANOVA based on Sørensen dissimilarities to test for differences in microbial community structure for the Main Tunnel (M), Pump Station (P) and the Test Site (T).

	df	SS	MS	Pseudo F	p
Between sites (M, P, T)	2	2.17	1.08	9.03	0.001
Residuals	61	7.32	0.12		
Total	63	9.49			
Between occasions, T	2	0.32	0.16	1.42	0.066
Residuals	20	2.24	0.11		
Total	22	2.56			
Between occasions, M	1	0.12	0.11	0.86	0.56
Residuals	7	0.90	0.13		
Total	8	1.02			
Between occasions, P	2	0.55	0.27	2.48	0.001
Residuals	29	3.20	0.11		
Total	31	3.75			

Notes: df = degrees of freedom; SS = sum of squares; MS = mean squares; Pseudo F = F value by permutation, p-values based on 999 permutations.
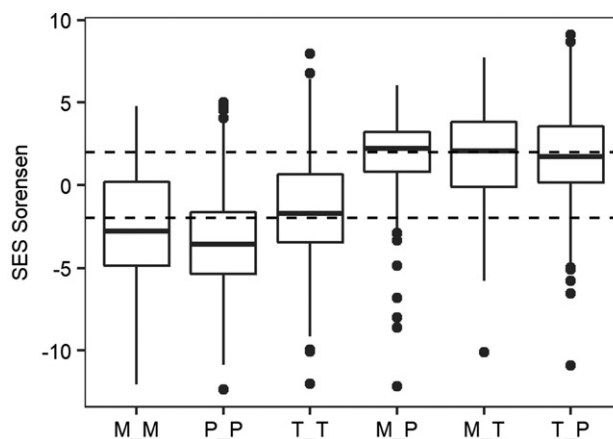

Figure 6. Standard effect size (SES) based on null-model predictions on the microbial communities in the Main Tunnel (M), Pump Station (P) and the Test Site (T). The three tests to the left show the SES within each site (M_M, P_P, T_T) and the three tests to the right show the SES between the sites (M_P, M_T, T_P). The hatched horizontal lines designate two SDs from the variation predicted by the null-model. The boxplot depicts the median (horizontal bold line); 25th and 75th percentiles (box delimiters); minimum and maximum values excluding outliers (vertical lines); and outliers (dots).

C-S-H, material loss and associated steel fibre corrosion. However, despite detailed documentation of sprayed concrete deterioration (see Hagelia 2011a), a mechanistic understanding of the underlying biological processes is lacking and data about microbial community structure on marine concrete surfaces are generally scarce. The composition of mature marine biofilms is affected by physical factors (light, temperature, water content and flow rate), chemical factors (pH, redox potential, the concentrations of eg DO, sulphide, nitrate and iron) and seasonal as well as geographical components affecting the local environment (Munn 2011). The effects of environmental

conditions on the assembly of microbial communities falls within deterministic factors, where selection shapes the microbial community due to differences in fitness among the organisms. It is well known that deterministic factors are important for microbial community assembly (Besemer et al. 2012; Delgado-Baquerizo et al. 2017). However, deterministic factors alone cannot explain the microbial diversity observed in nature and manmade systems. In many cases, considerable variation in microbial communities, such as biofilms, can be explained by stochastic factors through dispersal limitation, drift and diversification (Ofiteru et al. 2010; Zhou et al. 2013).

Here, the microbial composition, diversity and distribution were analysed for biofilms from three sites

Table 4. SEM-EDS analyses (atomic %) of the biofilm samples.

Point	O	C	Fe	Si	Cl	Na	Ca	S	Mg	Mn	M
1	20.1	24.8	37.6	7.1	3.6	1.7	2.3	0.5	0.4	0.5	2.3
2	22.5	32.5	28	6.8	3.1	1.9	1.9	0.6	0.5	0.7	1.9
3	28.7	27.6	25.1	9.4	2.9	1.8	1.7	0.4	0.5	0.3	1.7
4	37.7	30.6	18.4	5.1	2.5	2.7	1.3	0.4	0.4	ND	1.3
5	45.5	28.9	3.4	20.1	0.9	0.5	0.4	ND	ND	ND	0.4

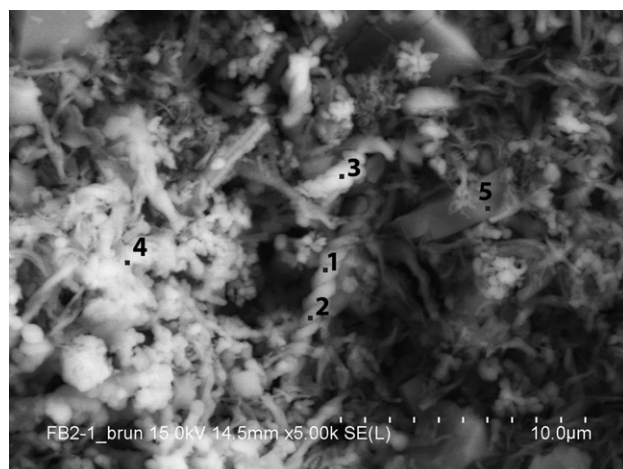Notes: M = minors. Analysed points correspond to Figure 7.

Figure 7. SEM back scatter micrograph of biofilm biomass. Analysis points 1–5 refer to measurements by EDS (see Table 4). Scale bar = 10 μm.

Figure 8. Parallel DO microprofiles from the biofilm–water interface (0 mm) measured at the pump station at local spots with different superficial water flow rate. Each data point shows the mean value and the SD ($n = 3$).

affected by concrete deterioration in the Oslofjord subsea tunnel, from November 2015 to October 2016. The samples of biofilm were collected from several locations at each site, subjected to water flow from different cracks in the concrete. Based on sequence analysis of the 16S rRNA genes, it was clear that the microbial communities at the three sites were different from each other, despite their geographical proximity, with <200 m between the sites. The separation between the sites was more pronounced with Sørensen dissimilarities giving equal weight to rare and abundant species (Figure 5, Table 3), suggesting that rare taxa had a major influence on the separation of communities. However, even with Bray–Curtis dissimilarities, giving a large weighting to abundant community members, the sites separated significantly (Figure S4, Table S3). Consequently, the variation in community structure between the tunnel sites was larger than the variation between different biofilm samples at each site (Table 3). Null-models were used to investigate whether these patterns were independent of the observed variation in richness (Figure 4) and at the same time to shed light on the mechanisms underpinning the microbial community assembly (Chase and Myers 2011; Stegen et al. 2012). SES confirmed that the separation between the tunnel sites
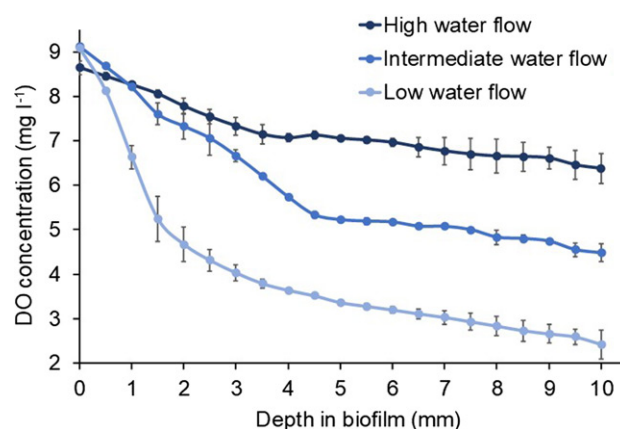
was larger than between the samples within each site (Figure 6). Analysis of nearest taxon index furthermore showed that the phylogenetic clustering of SVs in each sample of biofilm was significantly higher than would be predicted by chance (Figure S5). Such observations have been interpreted as evidence of deterministic habitat filtering (Webb et al., 2002; Horner-Devine and Bohannan 2006) where phylogenetically similar organisms share traits that would enable them to persist in given habitats (here the subsea tunnel biofilms). Between the tunnel sites, SES was higher than predicted by the null-model and within each site SES was lower. This finding suggests that deterministic forces were important for the assembly of the microbial communities (Chase and Myers 2011).

Data on the chemical composition of the influent water coming from the rock could not help in explaining the differences in microbial communities between the sites. However, in the samples of water after contact with biofilm, the concentrations of calcium, magnesium and vanadium showed significant fit to the ordination of the microbial community data (Table S4). It has been established that vanadium can leach from carbonated concrete (Müllauer et al.

2012). Interestingly, these metals were leaching from the concrete and biofilm surfaces to the water at all three sites (Table 1). Although indicating that leaching of these metals was linked to the microbial community structure differences, these observations need to be interpreted with caution due to the limited number of observations and warrant further investigation. Furthermore, the data on the chemical composition of the biofilm could not explain the microbial community data (Table S5). The concrete at the Main Tunnel and Pump Station had the same mix proportions (M45) and strength (B45) as the concrete at the Test Field, but differed in composition with addition of fly ash and polypropylene fibres to the Test Field concrete. Also, the concrete at the Test Field was sprayed more recently than the concrete at the other two sites. Comparative studies of biofouling on different concretes by indigenous microorganisms are scarce. Laboratory tests have shown differences in biogenic acid production, calcium dissolution and biofilm density on two types of concrete surfaces, suggesting different microbial colonisation patterns (Peyre Lavigne et al. 2015). Mineral properties of surfaces can certainly have a major effect on the composition and structure of microbial communities during colonisation caused by differences in mineral porosity and solubility as well as bioavailability of limiting nutrients (Uroz et al. 2015; Jones and Bennett 2017). However, for mature biofilms, the community structure is a result of multiple intricate abiotic and biotic interactions over time (Battin et al. 2016). In the Oslofjord tunnel, the biofilms developed over several years on variably degrading concrete at all three sites. Hence, the effect of the properties of the concrete on the community structure are uncertain.

The temperature of the seeping water was consistently higher at the Pump Station (13 °C) than at the Test Field and Main Tunnel (8–9 °C). Since different microorganisms have different temperature requirements, temperature can be expected to have affected the microbial community structure, although the magnitude remains unknown. Over large temperature ranges, microbial diversity has been shown to peak at mid-range, with lower diversity and concomitant changes in microbial composition at more extreme temperatures, consistent with the hypothesis that fewer species are adapted to such environments (Sharp et al. 2014; Wu et al. 2015). Smaller ranges of non-extreme temperatures, such as in this study, have however shown less conclusive effects on microbial communities. Clear effects on composition have been observed (Chong et al. 2018), but other studies have shown no or limited effects on diversity and composition and stronger effects of other environmental parameters (Fierer and Jackson 2006; Yergeau et al. 2012).

At all sites, the flow of water over the biofilm varied between different areas of the biofilm and between the three sites. In particular, the water flow was considerably greater at the Pump Station than at the other sites. Although not being measurable over an extensive biofilm area, these differences were easily observed both visually and by the time required to obtain water samples. At the Pump Station with its higher flow rate, the microbial communities were more dynamic over time than at the other sites (Table 3). Furthermore, the richness varied significantly between the sites, with the Pump Station having the lowest richness (Figure 4a). These two properties may well be linked, as larger richness has proven beneficial for community stability for many ecosystems including microbiota (Campbell et al. 2011; Tardy et al. 2014). It is well known that shear forces and mass transport by the water flow have a profound impact on biofilms (Stewart 2012). It can be hypothesised that the lower flow of water at the Main Tunnel and the Test Site would enable the establishment of more niches driving selection for a biofilm that would harbour a higher richness than the higher water flow at the Pump Station. The importance of superficial water flow rate for the DO concentrations in the biofilm was shown by the *in situ* microsensor measurements (Figure 8) and indicated a larger gradient of environmental conditions at the lower flow rates, and hence most likely more niches. Indeed, it has been shown that niche-differentiation caused by differences in hydrodynamic flow are important for biofilm community assembly (Besemer et al. 2009). However, the effects of flow patterns on microbial community structure may not be caused only by selection *via* niche-differentiation, since stochastic dispersal of microorganisms, from the water to the biofilm, could also have a considerable impact (Woodcock et al. 2013). But at heterogeneous flow conditions, for instance caused by rough and irregular surfaces such as sprayed concrete, dispersal has failed to explain community assembly patterns because of the formation of niches and concomitant selection (Woodcock et al. 2013; Battin et al. 2016).

Although differences in community structure between the three sites were evident, the composition of the communities was comparable with many shared abundant taxa (Figure 3). This observation suggests that in general, similar mechanisms

controlled the community assembly of microorganisms at the three sites. The microbial community composition of the subsea tunnel biofilms was different from the thoroughly investigated biofilms associated with concrete degradation in sewer pipes, where sulphur-oxidising and -reducing clades are numerically and functionally important contributors (Gomez-Alvarez et al. 2012; Cayford et al. 2017). The subsea tunnel communities had similarities in composition to sediments in the Oslofjord (Håvelsrud et al. 2012), as well as other marine sediments and biofilms (Choi et al. 2016; McBeth and Emerson 2016), with abundance of autotrophic nitrogen- and iron-oxidising microorganisms and several taxa of marine heterotrophic bacteria.

The ammonia-oxidising archaeon *Nitrosopumilus* sp. was observed at a particularly high abundance and ammonia-oxidising bacteria within the Nitrosomonadaceae were consistently detected. Nitrite-oxidising bacteria within *Nitrospina*, as well as *Nitrospira*, were also common, as were anammox bacteria within *Ca.* Scalindua. The autotrophic nitrogen converters were typically marine clades, well adapted to low substrate concentrations and able to tolerate low oxygen environments (Lücker et al. 2010; Park et al. 2010; Lücker et al. 2013) or anoxic conditions (Schmid et al. 2007), which may assist in explaining their abundance in the biofilms having a range of DO concentrations (Figure 8). Concrete deterioration associated with the activities of nitrifying bacteria has been observed in various concrete infrastructures (Cwalina 2008; Noeiaghaei et al. 2017). In the Oslofjord tunnel the nitrifiers may have contributed to the deterioration of the sprayed concrete, but only to certain degree given the low concentrations of nitrogen species in the water. Iron-oxidising bacteria of *Mariprofundus* sp. were detected in the biofilm at high abundance. They oxidise Fe(II) to Fe(III) at microaerophilic conditions and neutral pH, as was detected in the biofilm. During growth, *Mariprofundus* cells excrete extracellular stalks rich in polysaccharides and Fe(III). Such twisted stalks rich in iron were observed by SEM (Figure 7, Table 3), confirming their activity in the biofilm. The stalks are structures for deposition of metabolic products, which prevent cell encrustation and increase the solubility of Fe(II), thereby increasing the corrosion process (Chan et al. 2011; McBeth et al. 2011). The presence of *Mariprofundus* helps to explain the observed corrosion of the steel fibres in the sprayed concrete, the orange biofilm colour, and the high iron concentration in the biofilms (Table 2). The biofilm also contained high concentrations of precipitated manganese. However, no known manganese-oxidising bacteria were detected in the biofilms, as similarly observed in a preliminary investigation in the Oslofjord tunnel (Karačić et al. 2016). Yet, microorganisms resembling *Leptothrix discophora* were previously observed by SEM on samples collected at the Pump Station in 2005, when the water flow was much lower (Hagelia 2011a). Profound biogenic manganese oxidation has, however, been detected without identification of any known manganese-oxidising bacteria based on 16S rRNA gene sequences (Cao et al. 2015), suggesting that this trait is not only restricted to the phylogenetically diverse group of established manganese oxidisers. In addition, the biofilms contained a diversity of heterotrophic bacteria typically found in marine water and sediment including members of the marine benthic group JTB255 (Mußmann et al. 2017), Saprospiracae (McIlroy and Nielsen 2014), Kordiimonadaceae (Xu et al. 2014) and *Marinicella* (Rua and Thompson 2014). These organisms were presumably utilising the small bioavailable fraction of organic matter in the water as well as organic matter from internal cycling of biofilm components.

This study provides a first exploration of the microbial communities associated with concrete degradation in subsea tunnels. The communities at the three sites differed from each other, presumably influenced by deterministic factors where differences in water flow rate, temperature, concrete composition and leaching of calcium, magnesium and vanadium were identified as possible environmental gradients. Among the identified microbial taxa, a clear role of the omnipresent iron-oxidising bacterium *Mariprofundus* for the observed steel fibre corrosion could be established. Nitrifying- and heterotrophic bacteria presumably contributed to mild acidification and the thick biofilms likely caused locally high concentrations of metabolites which would promote concrete degradation, but the magnitude of these processes for the subsea tunnel deterioration remains uncertain. Moreover, many microbial taxa with hitherto unknown metabolism were present in the biofilm, pointing to the need for future detailed microbial studies to fully understand the underlaying mechanisms behind the observed biodeterioration.

Acknowledgements

University of Gothenburg, for providing support and use of their Illumina MiSeq.

ORCID

Frank Persson [iD] http://orcid.org/0000-0002-0269-9375

References

Albertsen M, Karst SM, Ziegler AS, Kirkegaard RH, Nielsen PH. 2015. Back to basics-the influence of DNA extraction and primer choice on phylogenetic analysis of activated sludge communities. PloS One. 10:e0132783 doi:10.1371/journal.pone.0132783

Bastidas-Arteaga E, Sánchez-Silva M, Chateauneuf A, Silva MR. 2008. Coupled reliability model of biodeterioration, chloride ingress and cracking for reinforced concrete structures. Struct Saf. 30:110–129. doi:10.1016/j.strusafe.2006.09.001

Battin TJ, Besemer K, Bengtsson MM, Romani AM, Packmann AI. 2016. The ecology and biogeochemistry of stream biofilms. Nat Rev Microbiol. 14:251–263. doi:10.1038/nrmicro.2016.15

Beech IB, Sunner J. 2004. Biocorrosion: towards understanding interactions between biofilms and metals. Curr Opin Biotechnol. 15:181–186. doi:10.1016/j.copbio.2004.05.001

Bertron A. 2014. Understanding interactions between cementitious materials and microorganisms: a key to sustainable and safe concrete structures in various context. Mater Struct. 47:1787–1806. doi:10.1617/s11527-014-0433-1

Besemer K, Peter H, Logue JB, Langenheder S, Lindström ES, Tranvik LJ, Battin TJ. 2012. Unraveling assembly of stream biofilm communities. Isme J. 6:1459–1468. doi:10.1038/ismej.2011.205

Besemer K, Singer G, Hodl I, Battin TJ. 2009. Bacterial community composition of stream biofilms in spatially variable-flow environments. Appl Environ Microbiol. 75:7189–7195. doi:10.1128/AEM.01284-09

Campbell V, Murphy G, Romanuk TN. 2011. Experimental design and the outcome and interpretation of diversity—stability relations. Oikos. 120:399–408. doi:10.1111/j.1600-0706.2010.18768.x

Cao LT, Kodera H, Abe K, Imachi H, Aoi Y, Kindaichi T, Ozaki T, Ohashi A. 2015. Biological oxidation of Mn(II) coupled with nitrification for removal and recovery of minor metals by downflow hanging sponge reactor. Water Res. 68:545–553. doi:10.1016/j.watres.2014.10.002

Caporaso JG, Lauber CL, Walters WA, Berg-Lyons D, Lozupone CA, Turnbaugh PJ, Fierer N, Knight R. 2011. Global patterns of 16S rRNA diversity at a depth of millions of sequences per sample. P Natl Acad Sci USA. 108:4516–4522. doi:10.1073/pnas.1000080107

Cayford BI, Jiang G, Keller J, Tyson J, Bond PL. 2017. Comparison of microbial communities across sections of a corroding sewer piper and the effects of wastewater flooding. Biofouling. 33:780–792. doi:10.1080/08927014.2017.1369050

Chan CS, Fakra SC, Emerson D, Fleming EJ, Edwards KJ. 2011. Lithotrophic iron-oxidizing bacteria produce organic stalks to control mineral growth: implications for biosignature formation. Isme J. 5:717–727. doi:10.1038/ismej.2010.173

Chase JM, Myers JA. 2011. Disentangling the importance of ecological niches from stochastic processes across scales. Philos Trans R Soc Lond, B, Biol Sci. 366:2351–2363. doi:10.1098/rstb.2011.0063

Choi H, Koh H-W, Kim H, Chae J-C, Park S-J. 2016. Microbial community composition in the marine sediments of Jeju Island: next-generation sequencing surveys. J Microbiol Biotechnol. 26:883–890. doi:10.4014/jmb.1512.12036

Chong CW, Silvaraj S, Supramaniam Y, Snape I, Tan IKP. 2018. Effect of temperature on bacterial community in petroleum hydrocarbon-contaminated and uncontaminated Antarctic soil. Polar Biol. 41:1763–1775. doi:10.1007/s00300-018-2316-3

Cwalina B. 2008. Biodeterioration of concrete. Acee J. 4:133–140.

Delgado-Baquerizo M, Reich PB, Khachane AN, Campbell CD, Thomas N, Freitag TE, Abu Al-Soud W, Sorensen S, Bardgett RD, Singh BK. 2017. It is elemental: soil nutrient stoichiometry drives bacterial diversity. Environ Microbiol. 19:1176–1188. doi:10.1111/1462-2920.13642

Edgar RC. 2010. Search and clustering orders of magnitude faster than BLAST. Bioinformatics. 26:2460–2461. doi:10.1093/bioinformatics/btq461

Fierer N, Jackson RB. 2006. The diversity and biogeography of soil bacterial communities. Proc Natl Acad Sci USA. 103:626–631. doi:10.1073/pnas.0507535103

Gaylarde CC, Morton LHG. 1999. Deteriogenic biofilms on buildings and their control: a review. Biofouling. 14:59–74. doi:10.1080/08927019909378397

Gomez-Alvarez V, Revetta RP, Santo Domingo JW. 2012. Metagenome analyses of corroded concrete wastewater pipe biofilms reveal a complex microbial system. BMC Microbiol. 12:122 doi:10.1186/1471-2180-12-122

Hagelia P. 2007. Sprayed concrete deterioration influenced by saline ground water and Mn-Fe biomineralisation in subsea tunnels. In: Jamtveit B, editor. Mechanical effects on reactive systems. The 20th Kongsberg Seminar. Oslo, Norway: PGP, University of Oslo; p 26.

Hagelia P. 2011a. Deterioration mechanisms and durability of sprayed concrete for rock support in tunnels [dissertation]. Delft, the Netherlands. TU Delft. https://repository.tudelft.nl/islandora/object/uuid:d64b8ff8-8d68-4eea-a320-73148e9f1b15/

Hagelia P. 2011b. Sprayed concrete in aggressive environment – the Oslofjord Test Site. In: Beck T, Woldmo O, Engen S, editors. Proceedings of the 6th international symposium on sprayed concrete—modern use of wet mix sprayed concrete for underground support, Tromsø, Norway, pp 161–175.

Harbulakova VO, Estokova A, Stevulova N, Luptáková A, Foraiova K. 2013. Current trends in investigation of

concrete biodeterioration. Procedia Eng. 65:346–351. doi: 10.1016/j.proeng.2013.09.053

Håvelsrud OE, Haverkamp TH, Kristensen T, Jakobsen KS, Rike AG. 2012. Metagenomic and geochemical characterization of pockmarked sediments overlaying the troll petroleum reservoir in the North Sea. BMC Microbiol. 12:203 doi:10.1186/1471-2180-12-203

Horner-Devine MC, Bohannan BJM. 2006. Phylogenetic clustering and overdispersion in bacterial communities. Ecology. 87:S100–S108. doi:10.1890/0012-9658(2006)87[100:PCAOIB]2.0.CO;2

Hugerth LW, Wefer HA, Lundin S, Jakobsson HE, Lindberg M, Rodin S, Engstrand L, Andersson AF. 2014. DegePrime, a program for degenerate primer design for broad-taxonomic-range PCR in microbial ecology studies. Appl Environ Microbiol. 80:5116–5123. doi:10.1128/AEM.01403-14

Hughes P, Fairhurst D, Sherrington I, Renevier N, Morton LHG, Robery PC, Cunningham L. 2013. Microscopic study into biodeterioration of marine concrete. Int Biodeter Biodegr. 79:14–19. doi:10.1016/j.ibiod.2013.01.007

Jones AA, Bennett PC. 2017. Mineral ecology: surface specific colonization and geochemical drivers of biofilm accumulation, composition, and phylogeny. Front Microbiol. 8:491. doi:10.3389/fmicb.2017.00491.

Karačić S, Hagelia P, Persson F, Wilén B. 2016. Microbial attack on subsea sprayed concrete. In: Wiktro V, Jonkers H, Bertron A, editors. The International Rilem Conference on Microorganisms-Cementitious Materials Interactions. Delft, Netherland: RILEM Publications SARL. p. 63–75.

Kembel SW, Cowan PD, Helmus MR, Cornwell WK, Morlon H, Ackerly DD, Blomberg SP, Webb CO. 2010. Picante: R tools for integrating phylogenies and ecology. Bioinformatics. 26:1463–1464. doi:10.1093/bioinformatics/btq166

Lücker S, Wagner M, Maixner F, Pelletier E, Koch H, Vacherie B, Rattei T, Damste JS, Spieck E, Le Paslier D. 2010. A Nitrospira metagenome illuminates the physiology and evolution of globally important nitrite-oxidizing bacteria. Proc Natl Acad Sci USA. 107:13479–13484. doi:10.1073/pnas.1003860107

Lücker S, Nowka B, Rattei T, Spieck E, Daims H. 2013. The genome of Nitrospina gracilis illuminates the metabolism and evolution of the major marine nitrite oxidizer. Front Microbiol. 4:27. doi: doi:10.3389/fmicb.2013.00027.

Magniont C, Coutand M, Bertron A, Cameleyre X, Lafforgue C, Beaufort S, Escadeillas G. 2011. A new test method to assess the bacterial deterioration of cementitious materials. Cement Concrete Res. 41:429–438. doi:10.1016/j.cemconres.2011.01.014

McBeth JM, Emerson D. 2016. In situ microbial community succession on mild steel in estuarine and marine environments: exploring the role of iron-oxidizing bacteria. Front Microbiol. 7:767. doi: doi:10.3389/fmicb.2016.00767.

McBeth JM, Little BJ, Ray RI, Farrar KM, Emerson D. 2011. Neutrophilic iron-oxidizing "zetaproteobacteria" and mild steel corrosion in nearshore marine environments. Appl Environ Microbiol. 77:1405–1412. doi:10.1128/AEM.02095-10

McIlroy SJ, Saunders AM, Albertsen M, Nierychlo M, McIlroy B, Hansen AA, Karst SM, Nielsen JL, Nielsen PH. 2015. MiDAS: the field guide to the microbes of activated sludge. Database (Oxford). 2015:bav062 doi:10.1093/database/bav062

McIlroy SJ, Nielsen PH. 2014. The family saprospiraceae. In: Rosenberg E, DeLong EF, Lory S, Stackebrandt E, Thompson F, editors. The Prokaryotes. Berlin Heidelberg: Springer; p. 863–889.

Müllauer W, Beddoe RE, Heinz D. 2012. Effects of carbonation, chloride and external sulphates on the leaching behaviour of major and trace elements from concrete. Cement Concrete Comp. 34:618–626. doi:10.1016/j.cemconcomp.2012.02.002

Munn CB. 2011. Marine microbiology: ecology and applications. New York: Garland Science.

Mußmann M, Pjevac P, Krüger K, Dyksma S. 2017. Genomic repertoire of the Woeseiaceae/JTB255, cosmopolitan and abundant core members of microbial communities in marine sediments. Isme J. 11:1276–1281. doi:10.1038/ismej.2016.185

Noeiaghaei T, Mukherjee A, Dhami N, Chae S-R. 2017. Biogenic deterioration of concrete and its mitigation technologies. Constr Build Mater. 149:575–586. doi:10.1016/j.conbuildmat.2017.05.144

Ofiteru ID, Lunn M, Curtis TP, Wells GF, Criddle CS, Francis CA, Sloan WT. 2010. Combined niche and neutral effects in a microbial wastewater treatment community. Proc Natl Acad Sci U S A. 107:15345–15350. doi:10.1073/pnas.1000604107

Okabe S, Odagiri M, Ito T, Satoh H. 2007. Succession of sulfur-oxidizing bacteria in the microbial community on corroding concrete in sewer systems. Appl Environ Microbiol. 73:971–980. doi:10.1128/AEM.02054-06

Oksanen JBF, Friendly M, Kindt R, Legendre P, McGlinn D. 2017. vegan: Community ecology package. https://cran.r-project.org/package=vegan

Park BJ, Park SJ, Yoon DN, Schouten S, Sinninghe Damste JS, Rhee SK. 2010. Cultivation of autotrophic ammonia-oxidizing archaea from marine sediments in coculture with sulfur-oxidizing bacteria. Appl Environ Microbiol. 76:7575–7587. doi:10.1128/AEM.01478-10

Peyre Lavigne M, Bertron A, Auer L, Hernandez-Raquet G, Foussard J-N, Escadeillas G, Cockx A, Paul E. 2015. An innovative approach to reproduce the biodeterioration of industrial cementitious products in a sewer environment. Part I: test design. Cement Concrete Res. 73:246–256. doi:10.1016/j.cemconres.2014.10.025

Rua CPJ, Thompson F. 2014. The unclassified genera of Gammaproteobacteria: Alkalimonas, Arenicella, Chromatocurvus, Congregibacter, Gallaecimonas, Halioglobus, Marinicella, Methylohalomonas, Methylonatrum, Orbus, Plasticicumulans, Porticoccus, Sedimenticola, Simiduia, Solimonas. In: Rosenberg E, DeLong EF, Lory S, Stackebrandt E, Thompson F, editors. The Prokaryotes. Berlin Heidelberg: Springer; p. 749–768.

Schmid MC, Risgaard-Petersen N, van de Vossenberg J, Kuypers MM, Lavik G, Petersen J, Hulth S, Thamdrup B, Canfield D, Dalsgaard T. 2007. Anaerobic ammonium-oxidizing bacteria in marine environments: widespread occurrence but low diversity. Environ Microbiol. 9:1476–1484. doi:10.1111/j.1462-2920.2007.01266.x

Sharp CE, Brady AL, Sharp GH, Grasby SE, Stott MB, Dunfield PF. 2014. Humboldt's spa: microbial diversity is controlled by temperature in geothermal environments. Isme J. 8:1166–1174. doi:10.1038/ismej.2013.237

Stegen JC, Lin XJ, Konopka AE, Fredrickson JK. 2012. Stochastic and deterministic assembly processes in sub-surface microbial communities. Isme J. 6:1653–1664. doi: 10.1038/ismej.2012.22

Stewart PS. 2012. Mini-review: convection around biofilms. Biofouling. 28:187–198. doi:10.1080/08927014.2012.662641

Stoodley P, Boyle JD, DeBeer D, Lappin-Scott HM. 1999. Evolving perspectives of biofilm structure. Biofouling. 14: 75–90. doi:10.1080/08927019909378398

Tardy V, Mathieu O, Lévêque J, Terrat S, Chabbi A, Lemanceau P, Ranjard L, Maron P-A. 2014. Stability of soil microbial structure and activity depends on micro-bial diversity. Environ Microbiol Rep. 6:173–183. doi: 10.1111/1758-2229.12126

Taylor HFW. 1997. Cement chemistry. (2nd ed.). London: Thomas Thelford Publishing.

Torres-Luque M, Bastidas-Arteaga E, Schoefs F, Sánchez-Silva M, Osma JF. 2014. Non-destructive methods for measuring chloride ingress into concrete: state-of-the-art and future challenges. Constr Build Mater. 68: 68–81. doi:10.1016/j.conbuildmat.2014.06.009

Uroz S, Kelly LC, Turpault M-P, Lepleux C, Frey-Klett P. 2015. The Mineralosphere concept: mineralogical control of the distribution and function of mineral-associated bacterial communities. Trends Microbiol. 23:751–762. doi:10.1016/j.tim.2015.10.004

Webb CO, Ackerly DD, McPeek MA, Donoghue MJ. 2002. Phylogenies and community ecology. Annu Rev Ecol Syst. 33:475–505. doi:10.1146/annurev.ecolsys.33.010802.150448

Woodcock S, Besemer K, Battin TJ, Curtis TP, Sloan WT. 2013. Modelling the effects of dispersal mechanisms and hydrodynamic regimes upon the structure of microbial communities within fluvial biofilms. Environ Microbiol. 15:1216–1225. doi:10.1111/1462-2920.12055

Wu J, Xiong J, Hu C, Shi Y, Wang K, Zhang D. 2015. Temperature sensitivity of soil bacterial community along contrasting warming gradient. Appl Soil Ecol. 94:40–48. doi:10.1016/j.apsoil.2015.04.018

Xu XW, Wu M, Oren A. 2014. The family kordiimonada-ceae. In: Rosenberg E, DeLong EF, Lory S, Stackebrandt E, Thompson F, editors. The Prokaryotes. Berlin Heidelberg: Springer; p. 307–312.

Yergeau E, Bokhorst S, Kang S, Zhou J, Greer CW, Aerts R, Kowalchuk GA. 2012. Shifts in soil microorganisms in response to warming are consistent across a range of ant-arctic environments. Isme J. 6:692–702. doi:10.1038/ismej.2011.124

Zhou JZ, Liu WZ, Deng Y, Jiang YH, Xue K, He ZL, Van Nostrand JD, Wu LY, Yang YF, Wang AJ. 2013. Stochastic assembly leads to alternative communities with distinct functions in a bioreactor microbial community. mBio. 4:e00584–e00512.